PICOMETER RESOLUTION HETERODYNE INTERFEROMETRY FOR SHORT TO MEDIUM TERM DIMENSIONAL STABILITY MEASUREMENTS

A.S. van de Nes, D. Voigt

VSL Dutch Metrology Institute, Thijsseweg 11, 2629 JA Delft, The Netherlands

ABSTRACT

A thorough understanding of dimensional drift phenomena at the picometer range, stemming from ageing, temperature changes or mechanical stresses in instrumentation or the object to be measured, is essential for high-end precision engineering and accurate measurements. For that purpose, a balanced double-sided heterodyne interferometer is developed to perform traceable measurements of dimensional drift with an uncertainty of less than 10 pm at the short-term (seconds to minutes), and 100 pm at the medium-term (hours to days).
The performance of the instrument is presented by means of a 66 hour long double dead-path difference measurement, demonstrating the desired uncertainty levels during a selected period of 19 hours, while operating in ambient air conditions. The residual pressure related path length difference fluctuations form the current limitation to the measurement uncertainty.

Index Terms - dimensional stability, picometer uncertainty, optical metrology, displacement interferometry

1. INTRODUCTION

For high-end precision engineering and accurate measurements, a thorough understanding of dimensional drift phenomena at the picometer range is essential. Particularly the aerospace and ICT industry are critically limited in system performance due to minute material and material-connection drifts. These dimensional drift effects stem from ageing, temperature changes or mechanical stresses in instrumentation or the object to be measured. Following up on an earlier cooperation with Delft Technical University and TNO [1], VSL has continued the development of a facility to investigate and quantify dimensional drift by contactless means with tens of picometer accuracy during hours of measurement time. The research required for the facility, denoted the “Picodrift instrument”, to reach this goal is performed as part of the European Metrology Research Programme (EMRP) project “Thermal design and dimensional drift (IND13)” [2].
With the completion of the work of J.D. Ellis [3], the Picodrift instrument was moved to VSL and prepared for traceable dimensional metrology use. To improve the performance of the instrument further, additional research was required for reaching the goal of an uncertainty of less than 10 pm at the short-term (seconds to minutes), and 100 pm at the medium-term (hours to days). In this document, we address the contribution to the drift measurement from the remaining thermal fluctuations on the alignment, as well as the dependence on a pressure sealed, and even preferably evacuated, sample environment. Also, to maximise the signal-to-noise ratio of detector and electronics, more laser power was made available to the instrument. The effect on the performance of the instrument of selected individual optical components was analysed, and the data processing methodology was modified. Finally, we present a double dead-path measurement to characterise the current performance of the instrument.

2. PICODRIFT INSTRUMENT

2.1 Picodrift instrument overview

The photograph shown in Figure 1, presents an overview of the Picodrift instrument operating in ambient air. The measurement and control instrumentation is placed in and on top of the rack next to the optical table. The laser, several optical detectors, the electro-optic modulator (EOM), the acousto-optic modulators (AOMs), the camera, and the required optical components for manipulation of the laser beam have been placed on top of a high quality optical table with excellent vibration isolators. The temperature in the lab is controlled to better than 0.1 K stability, and the lab-conditions are monitored and documented. The two aluminium foil covered boxes provide additional thermal shielding for the ultra low expansion (ULE) reference cavity (small box), and the Picodrift interferometer (large box).

Figure 1: Overview of the Picodrift instrument. The control and measurement instrumentation is placed in and on top of the rack next to the optical table. The diode laser, several detectors, electro-optics modulator (EOM), acousto-optic modulators (AOMs), camera, and the required optical components for manipulation of the laser beam are positioned on top of the optical table. The ULE reference cavity (smaller box), and the Picodrift interferometer (larger box), are located inside two aluminium foil covered boxes providing additional thermal shielding.

In Figure 2, a schematic representation of the Picodrift instruments is shown. The light is provided by an external cavity diode laser, which is frequency locked against a stable, thermally shielded, ULE reference cavity (highlighted by the purple block) housed inside a not-evacuated vacuum tube in order to dampen pressure fluctuations. The oscillation frequency is measured using a counter by observing the beat note signal of the instrument laser with an iodine stabilized HeNe standard laser (highlighted by the green block). The actual dimensional difference measurements are performed by interfering two laser beams travelling almost identical paths with a slightly detuned frequency ($\Delta f = f_1 - f_2$), in order to track the changes in phase, and therefore path-length, between the two beams (highlighted by the pink block). The interferometer is placed inside its own thermally shielded box, with all heat producing components removed. Additionally, to monitor and potentially correct for effects due to residual thermal, pressure, or refractive index fluctuations, the interferometer

environment is measured using several thermistors and a pressure sensor close to the studied sample. A more detailed description of the individual components is given in the following sections.

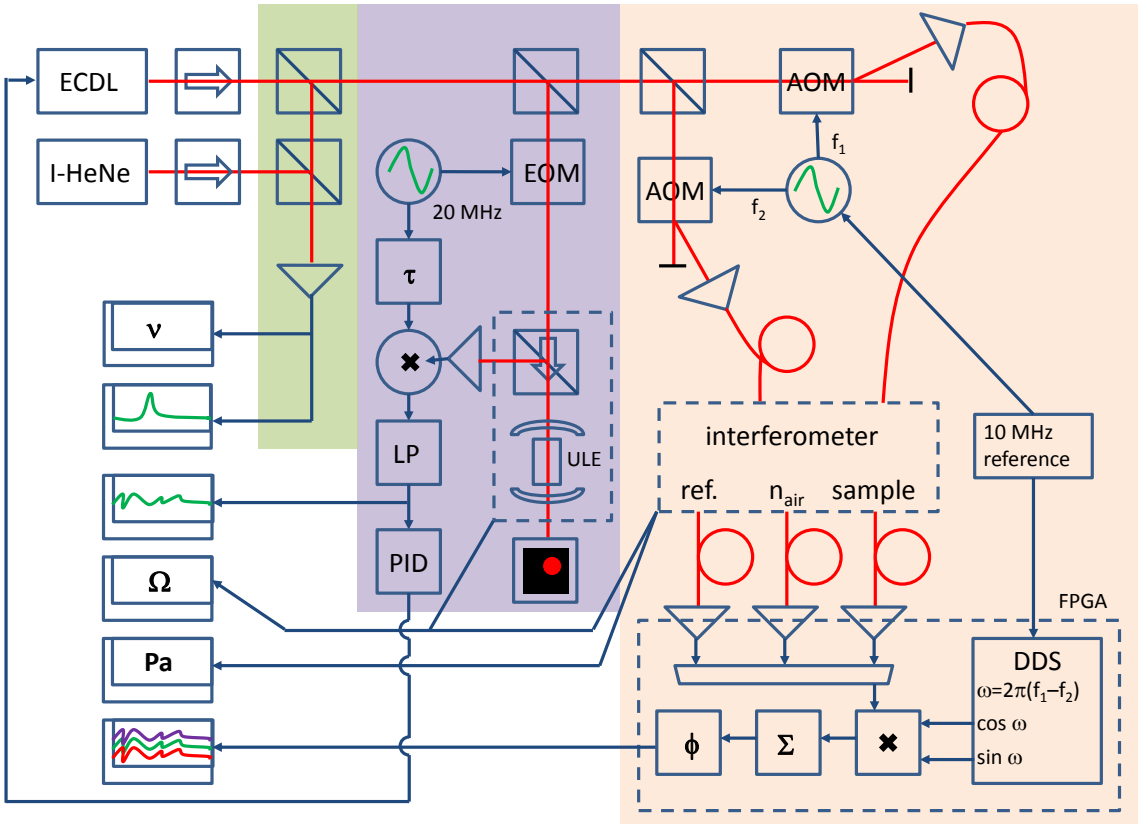

Figure 2: Schematic representation of the Picodrift instrument, developed to measure dimensional drift at the picometer range. The external cavity diode laser (ECDL) provides the light used for the interferometer. First, highlighted by the green block, part of the light is split off for measuring the frequency of the beat note with an iodine stabilized HeNe standard laser using a counter. Next, highlighted by the purple block, part of the light is split off to lock the laser frequency against a stable reference cavity. Last, highlighted by the pink block, two fibers deliver the laser light, oscillating at slightly detuned frequencies, to the interferometer, and any change in dimension of the sample under study is registered by the FPGA based detection routine.

2.2 Laser stabilisation and beat detection

In Figure 3, the optical and electronic components placed on the optical table are displayed, which are required for the laser beam preparation, delivery, and detection. As the main light source, an external cavity diode laser from New Focus (Vortex TLB-7004 with 633 nm diode) with abundant laser power is used, followed by an optical isolator, half-wave plate, anamorphic prism pair, and steering mirror, before coupling into a polarization maintaining fiber. The laser is based on a thermally controlled Littman-Metcalf piezo controlled external cavity design. The frequency of the laser can be coarsely tuned using the piezo control, and finely tuned by adjusting the driving current. Alternatively, a stabilized HeNe laser from Melles-Griot (25STP912-230) with 1 mW output power is available, or a fiber coupled distributed Bragg reflector laser from Eagleyard (EYP-DBR-0633-00005-2000-BFY02-0000) can be similarly locked to the reference cavity.

The light from the selected laser is directed through an optical isolator, positioned at the bottom centre of Figure 3, and is divided in to a path toward the beat note detection and reference cavity, or to the interferometer, by means of a half-wave plate and polarising beam splitter. The path to the beat note detection is split off from the path to the reference cavity by means of another half-wave plate and polarising beam splitter. The light toward the reference

cavity passes through an electro-optic modulator (EOM) and is coupled in to a polarisation maintaining fiber using two beam steering mirrors.

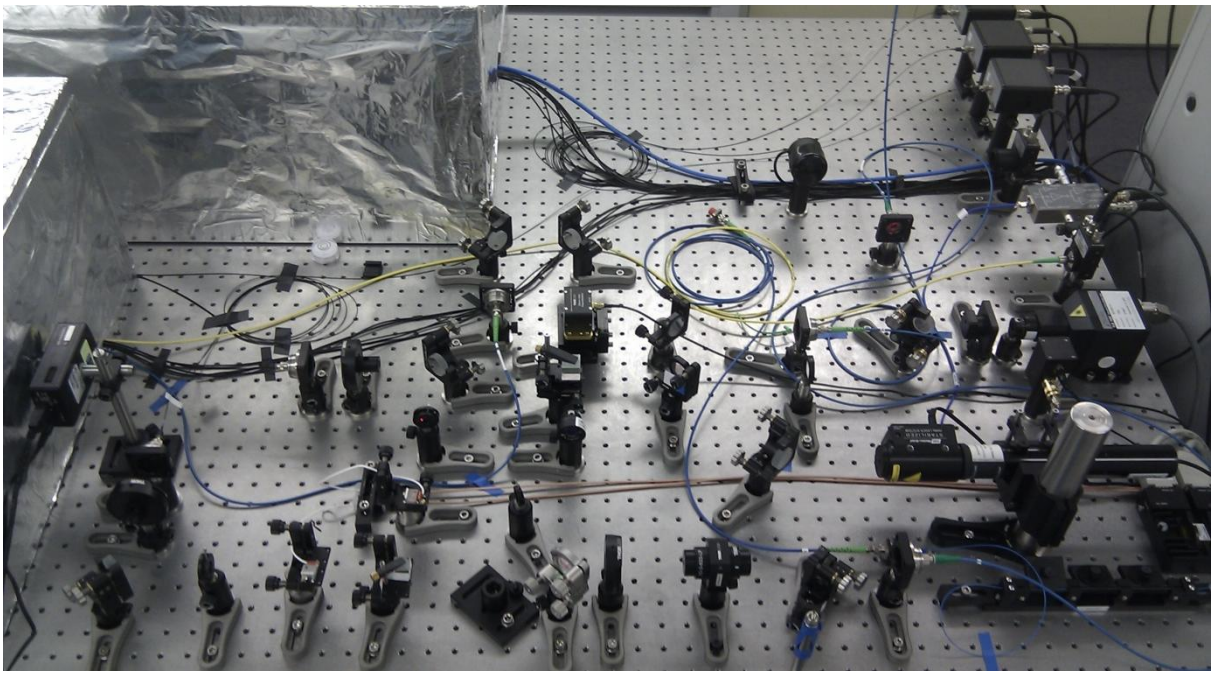

Figure 3: Optical components required for preparation, delivery and detection of the laser light. Lasers and detectors are located at the right of the table. In the centre, the EOM and AOMs can be found, and on the left, the shielding boxes for the interferometer and reference cavity are placed.

The laser frequency is locked to a homebuilt reference cavity, see Figure 4, where an ULE spacer separates two fused silica mirrors to form a 14 cm long Fabry-Pérot cavity, and the assembly is housed in a pressure damped vacuum tube. The vacuum tube is mounted on a small breadboard and placed in a thermally shielded aluminium foil covered box (single layer 2 cm thick extruded polystyrene foam). The temperature gradients inside the box are monitored by 5 thermistors. The laser frequency is locked on the zeroth order cavity mode using a Pound-Drever-Hall (PDH) technique. The laser light, including the 20 MHz side bands generated by the EOM, is delivered to the breadboard by a polarisation maintaining fiber, passes through an optical isolator, a half-wave plate, mode matching lens and steering mirrors before entering the Fabry-Pérot cavity. The reflected beam returns along the same path up to the optical isolator, where it passes through the exit port and is coupled in to a single mode fiber connected to an optical detector. The transmitted beam passes through the box via two colour filters, and is displayed on a camera. The Allan deviation of the locked frequency results in a minimum deviation of less than 10 kHz between 1 to 45 s averaging times, corresponding to less than 2 pm uncertainty. The long term frequency changes are monitored using the beat note measurements.

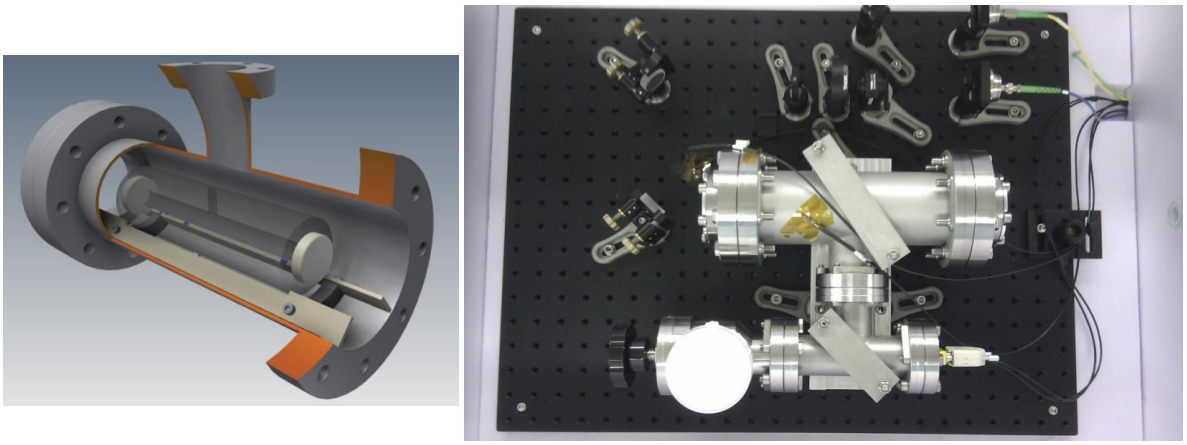

Figure 4: 3D model of the ULE reference cavity (left), and photograph of the optical components and vacuum tube housing of the reference cavity inside the thermally shielding aluminium foil covered box (right).

The beat note measurement is performed by overlapping the laser light from the diode laser with the light from an iodine stabilised HeNe standard laser, delivered to the optical table by another polarisation maintaining fiber. The beat note signal is detected by an optical detector and measured by a frequency counter referenced to the in house 10 MHz clock frequency standard, as well as displayed on a spectrum analyser for visualisation of the beat note signal.

2.3 The Picodrift interferometer

As can be observed in Figure 3, the optical path toward the interferometer passes first through a non-polarising beam splitter, before both light beams encounter an acousto-optic modulator (AOM) and a polariser and are coupled in to a polarisation maintaining fiber. Next, the polarisation maintaining fiber delivers the light to the Picodrift interferometer, shown in Figure 5, housed inside a second thermally shielding box. The two 40 MHz signals driving the AOMs are generated by an arbitrary waveform generator (LeCroy Arbstudio 1104) which is referenced to the in house 10 MHz clock frequency standard. The difference frequency between both signals has been carefully evaluated for its contribution to the overall noise level. To minimise the effect of acoustical vibrations from the fibers, a difference frequency of 1.5 MHz has been selected. After delivery to the interferometer bench, another polariser cleans-up potential polarisation mixing that can occur in the optical fiber. The polariser outside the shielding box is aligned such that the extinction rate is maximised, as can be evaluated by making a full rotation of the polariser inside the box. Afterwards the polariser inside the box is rotated such in order to align the polarisation with the optical axis of the polarising beam splitters of the interferometer.

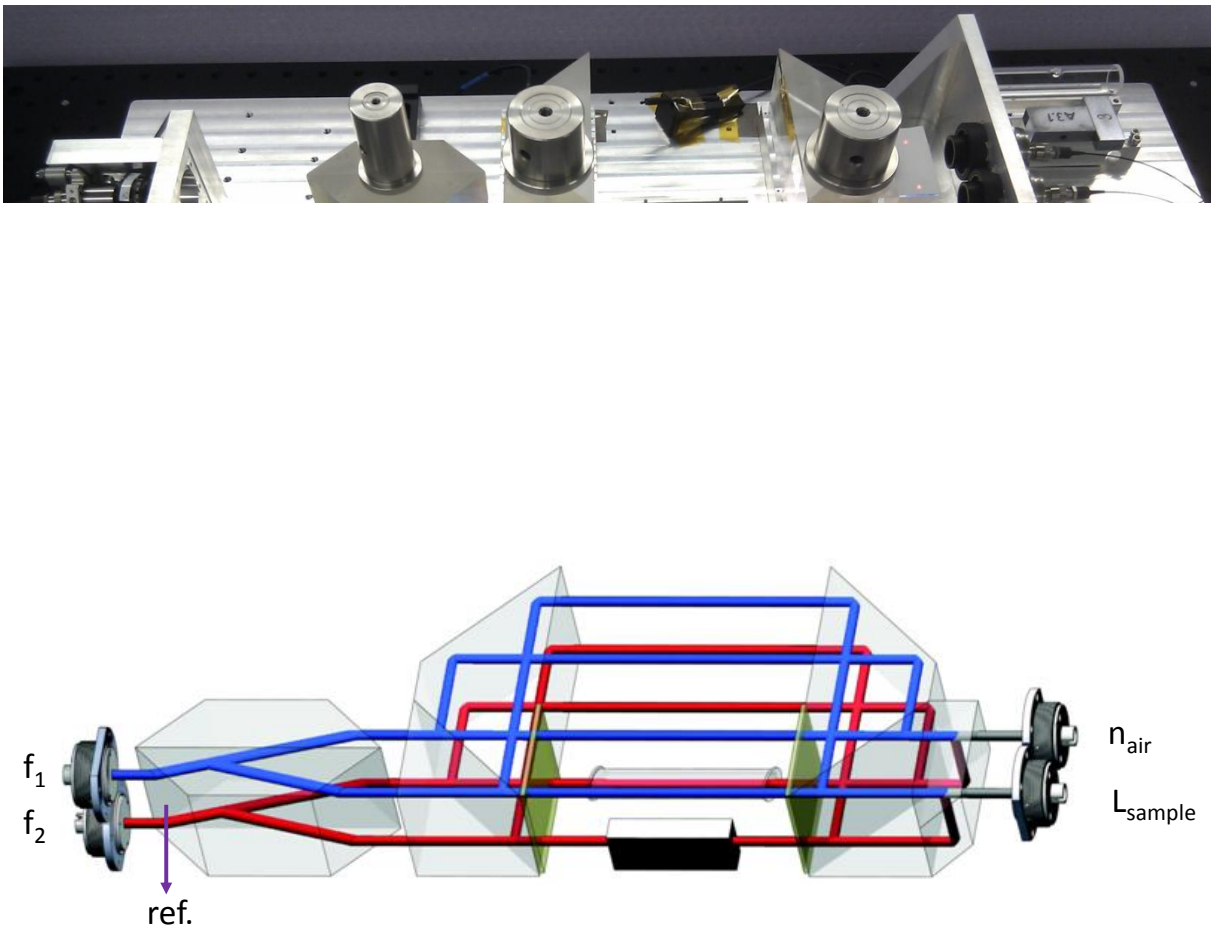

Figure 5: Photograph (top) and schematic representation (bottom) of the balanced double-sided heterodyne interferometer. For reference, the refractometer cell and a sample consisting of two wrung gauge blocks are shown in the right top of the photograph. From left to right, the laser light is delivered to the fiber couplers, cleaned up by polarisers, pass through a non-polarising beam splitter, polarising beam splitter, quarter-wave plate, sample or refractometer cell, another quarter-wave plate, a secondary polarising beam splitter, a lateral displacement beam splitter, and ultimately, the fiber couplers connected to the optical detector. The reference signal is obtained from the reflection at the first surface of the non-polarising beam splitter.

The temperature gradients and pressure fluctuations inside the box shielding the Picodrift interferometer are monitored using 10 thermistors and a pressure sensor. The thermally shielding box consists of two layers of 2 cm thick extruded polystyrene foam, sandwiching a thin metal sheet, present for homogenising any remaining temperature gradients. The box is covered by aluminium foil to reduce the influence of thermal radiation. The thermal performance of the box results in temperature gradients below 1 mK/h after a 24h period of acclimatisation.

The interferometer is designed such, that as much as possible common-path contributions are systematically excluded from the measurement signal. The optical components forming the interferometer are placed on top of a single block of aluminium, and all platforms are made of the same material. Two beams are delivered to the interferometer propagating parallel to each other but displaced in vertical direction, and detuned by the selected difference frequency. A non-polarising beam splitter is used to generate one optical branch for detection of the changes in dimension of the sample, and one optical branch for the refractometer used to correct for refractive index fluctuations. The signal reflected from the first surface of the beam splitter is coupled into an optical fiber, and used to generate the reference signal which inhibits all path length variations up to the beam splitter, and hence can be removed from the interferometer signals. Next, the light passes through a polarising beam splitter in

combination with a quarter-wave plate. The circularly polarised light is reflected from the sample, or passes through the refractometer cell (lower beams), or through free space (upper beams). Another quarter-wave plate returns the polarisation state back to linear, albeit orthogonally polarised to the initial state. Now the light is reflected by a polarising beam splitter, passes through the parallel path opposite to the sample and vacuum cell, and is reflected by another polarising beam splitter. Lastly, the light passes once more through the quarter-wave-plate, reflects from the sample or passes through the refractometer cell, and passes through the quarter-wave plate. Finally the polarisation state of the light is back to its original orientation, and the beam leaves the interferometer through the secondary polarising beam splitter. A lateral displacement beam splitter recombines for both branches the upper and lower beams with slightly detuned frequencies, and the light containing the desired interference signal is coupled into an optical fiber.

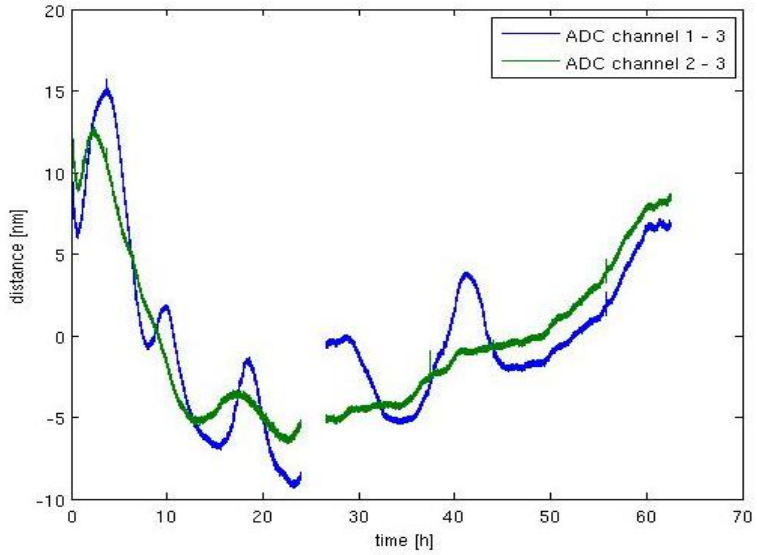

Figure 6: Preliminary double dead-path measurement results demonstrating the recorded path length variations in nanometers as a function of the time in hours at ambient air conditions. The path length difference is displayed with respect to the reference signal, where the optical branch for the sample is depicted in blue, and for the refractometer is depicted in green.

An initial double dead-path test measurement, shown in Figure 6, demonstrates a slowly oscillating path length variation of several nanometres, most dominantly visible in the optical branch of the sample, which can be related to the temperature gradient. At first, the effect was believed to be caused by rotation of the non-polarising beam splitter, but fixating the orientation by the addition of a spring loaded plunger did not resolve the unwanted oscillations. Next, suspicions regarding the pointing stability of the fiber couplers (Thorlabs PAF-X-11) delivering the beams to the interferometer have been proven false, as replacing them with fiber collimators (Thorlabs TC12APC-633) held by a low drift mirror mount (Thorlabs Polaris-K05S2) resulted in a similarly oscillating signal. Ultimately, the oscillations turned out to be caused by rotation of the polarising beam splitters due to the contact with the adjustment screws. This has been resolved by retracting the adjustment screw after the correct alignment was established.

2.4 Electronic phase detection

The interference signal, approximately oscillating at the predetermined 1.5 MHz difference frequency, is detected by three 125-MHz, low noise, photo-receivers. The signal is filtered and amplified further before being transferred to the 4 channel 120 MS/s analog-to-digital

converter (NI 5734). The algorithm to translate the electronic signal in to optical path length differences is executed by a fast field-programmable gate array (FPGA) from National Instruments (NI PXIe-7962R), which allowed for programming in LabVIEW. As the FPGA clock frequency is locked to the in house 10 MHz clock frequency standard, a direct digital synthesised 1.5 MHz reference frequency can be used to acquire the multiplication of the cosine and sine reference signals with the respective sample, refractometer and reference signals. These components are averaged over an integer times the reference period, and afterwards converted into intensity and phase values. In order to reduce the data rate and improve the signal-to-noise ratio, an Allan deviation analysis has been performed, yielding a minimum deviation at a rate of 8 S/s. Since a slightly higher data rate is desirable, the signals are averaged over 4,000,000 samples, or 50,000 periods, to arrive at a 30 S/s sample rate. The contribution of the electronic noise to the uncertainty in path length variations is of the order of 1 pm.

3. DOUBLE DEAD-PATH MEASUREMENT

To characterise the performance of the improved Picodrift instrument, a double dead-path measurement has been performed, where the sample and refractometer cell have been removed from the interferometer. The measurement was initially started with the polarising beam splitters in contact with the adjustments screws. After 22 hours of measurement time the box was opened and the adjustment screws retracted, removing the slow temperature dependent oscillations from the differential signal. The continued measurement data is shown from 23 hours onward in Figure 7, where the remaining settling time required for relaxing the critical temperature gradients after opening of the box is still visible during the first few hours. Note, to reduce the post-processing time, only data points at a 1 s interval are shown, discarding the remaining data points recorded at a rate of 30 S/s. Between approximately 60 and 64 hours after starting the measurement, the PID controller reached its voltage limit of 10 V, and the laser frequency lock was released. During this period, the free running laser displayed frequency oscillations of the order of 200 MHz, after which the laser was relocked. The double dead-path signal, i.e. the difference between the two interferometer branches, shows prolonged periods of good stability in between some relatively strong temperature and pressure induced length changes.

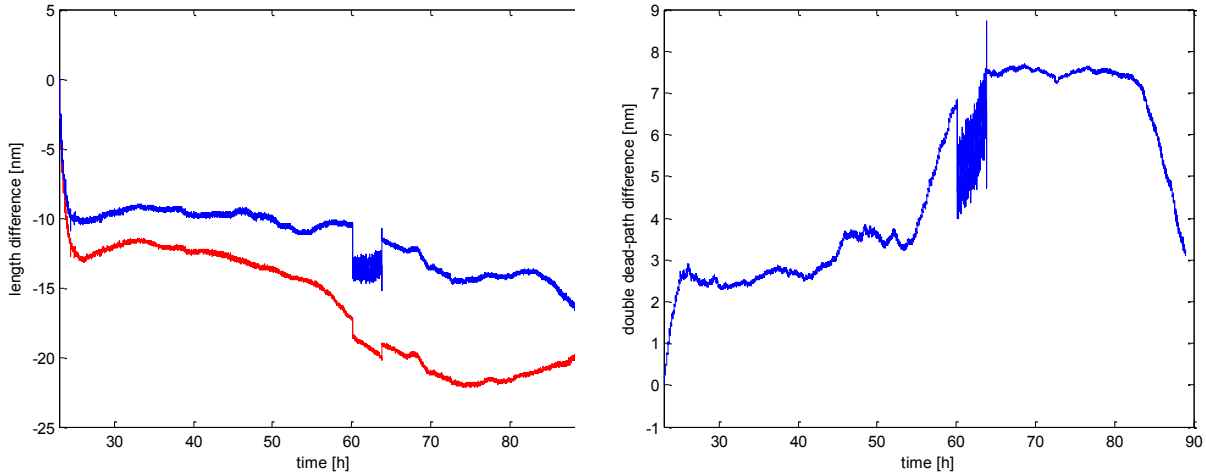

Figure 7: Length difference (left) as recorded for the two empty branches of the interferometer with respect to the reference signal reflected from the non-polarising beam splitter (blue for the sample branch, and red for the refractometer branch). The differential between the two signals (right) shows periods of good stability in between some relatively strong temperature (start of the curve) and pressure induced length changes.

The environment conditions during the measurement are shown in Figure 8. The refractive index changes, as calculated using the modified Edlén equation, are almost entirely determined by the pressure fluctuations. The beat note frequency follows a gentle slope of about 250 kHz/h. Although a correction can be easily performed using the frequency data recorded by the counter, evacuating the reference cavity might remove the need for such a correction. The thermistors inside the box shielding the interferometer display a gradient of less than 0.5 mK/h, and a maximum temperature difference between them of about 5 mK, excluding the less relevant breadboard sensor. The thermistors in the single layered box shielding the reference cavity display a gradient of 2 mK/h, and about 10 mK difference between the air temperature in front of and inside the not-evacuated vacuum tube.

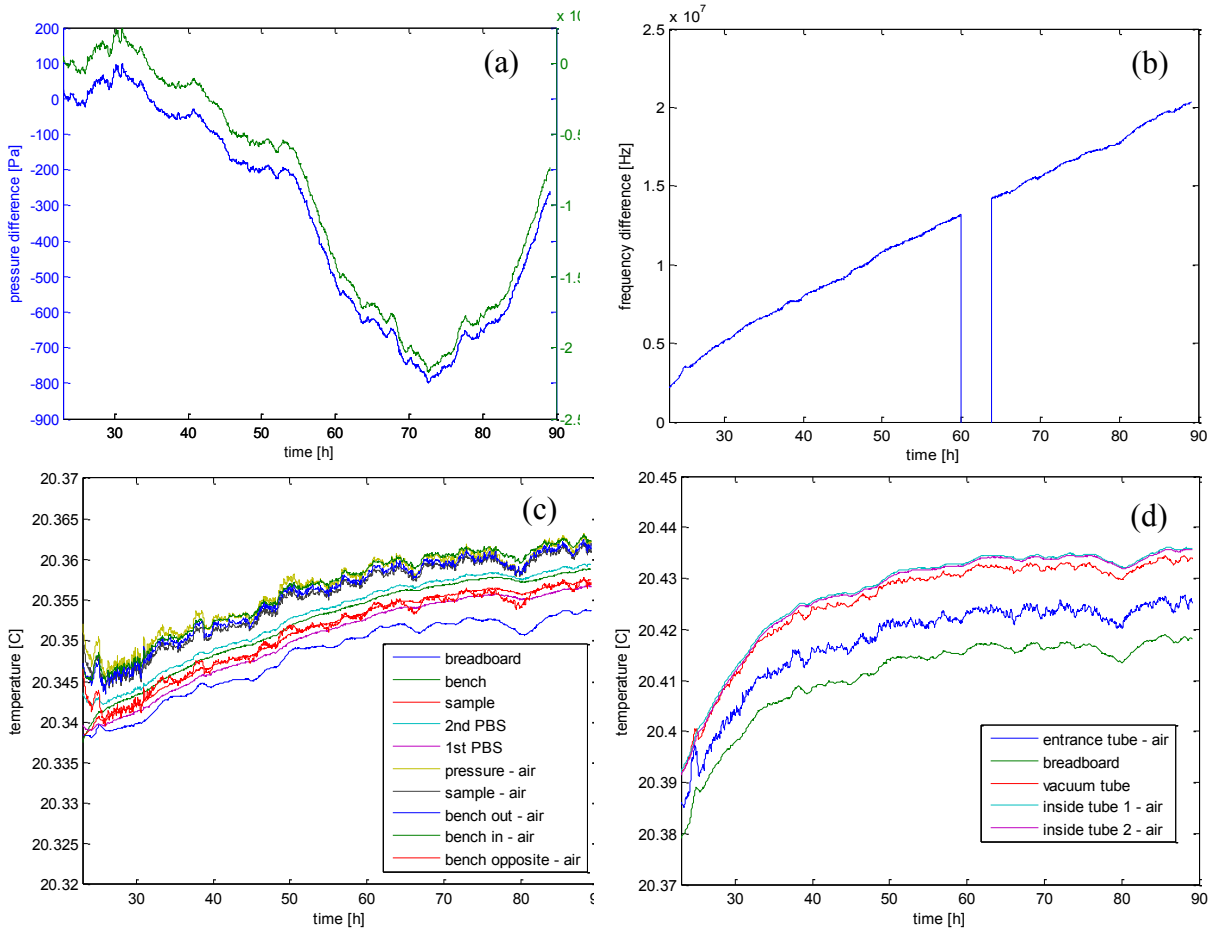

Figure 8: (a) Pressure in Pa (left axis) and refractive index (right axis) difference as calculated using the modified Edlén equation, (b) frequency difference in Hz, (c) temperature in °C inside the box shielding the interferometer, and (d) temperature in °C inside the box shielding the ULE reference cavity, as a function of time.

The two periods of steep increase and decrease of the double dead-path difference, Figure 7, shows a strong correlation with the rapid pressure fluctuations of about 300 Pa in 6 hours. When concentrating on the measurement data in between these events, as shown in Figure 9, a 19 hour long period with a relatively stable double dead-path difference is demonstrated. The remaining fluctuations still show a strong correlation with the pressure fluctuations, and might be corrected for. Further study has to indicate the exact origin of these fluctuations, but a first analysis indicates in the direction of an asymmetry in the compression of the (asymmetric) polarising beam splitters, and therefore a residual path length difference.
In Figure 10 the root mean square average over a time interval of 1 minute (blue) and 1 hour (red) along the 66 hour measurement time-span is shown. The interval between 64 and 83

hours demonstrates a standard deviation of the short term fluctuations (1 minute) of less than 22 pm, and for the medium-term fluctuations (1 hour) of the order of 40 pm. Over the entire 19 hour period, the standard deviation is 88 pm, and the peak-to-peak difference is just below 0.5 nm. The amplitude spectrum displayed it the right graph of Figure 10 shows a very good performance of the instrument for periods up to tens of minutes for the entire time-span to a few hours for the 19 hour sub-selection operating at ambient air conditions.

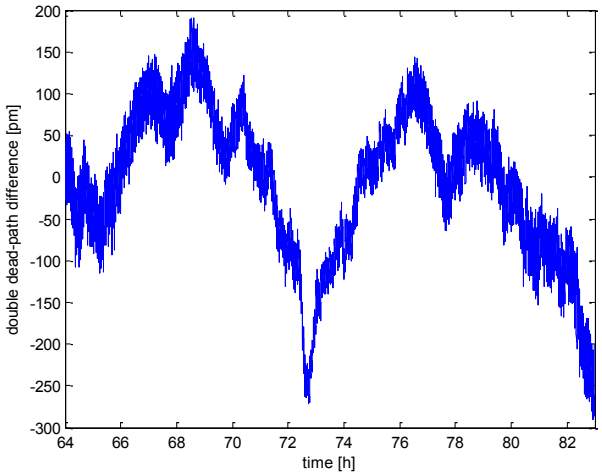

Figure 9: Sub-selection of the data shown in the right graph of Figure 7, during a period with a moderate contribution of pressure induced length changes. The correlation with the pressure fluctuations is still apparent and might be corrected for. The difference signal during the 19 hour period has a standard deviation of 88 pm and peak-to-peak value of slightly less than 0.5 nm.

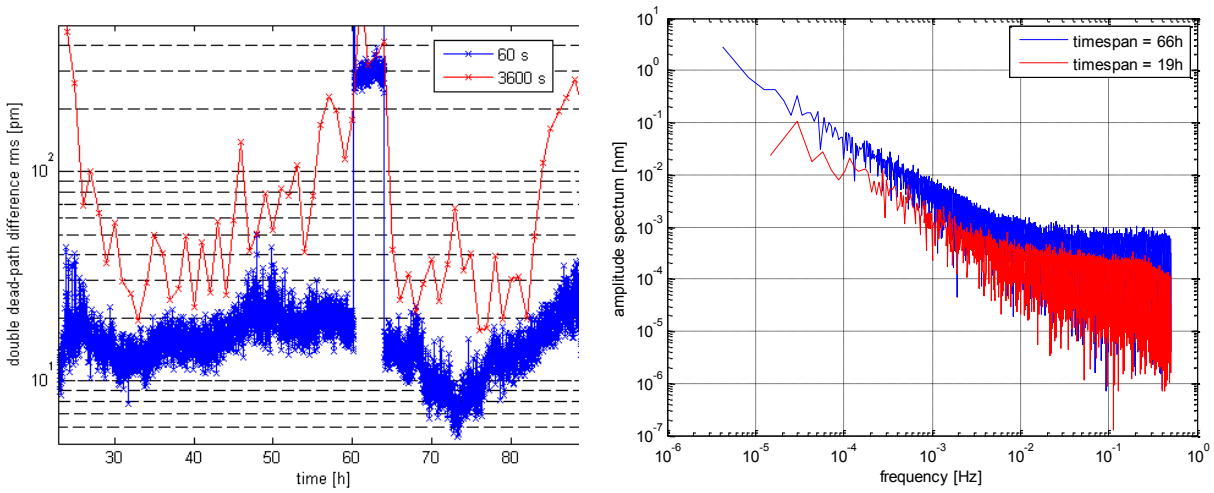

Figure 10: Root mean square average (left) as a function of time for the entire available data (>7.1 million samples) of the double dead-path difference over a 60 s interval (blue) and 3600 s interval (red), respectively. Amplitude spectrum (right) of the 66 hour time-span (blue), and the 19 hour sub-selection (red) as a function of the frequency, note that for the amplitude spectrum only the reduced data set has been used restricting the maximum frequency to 0.5 Hz.

4. CONCLUSION

A balanced double-sided heterodyne interferometer, denoted the “Picodrift instrument”, designed to operate with a measurement uncertainty of less than 10 pm at the short-term (seconds to minutes), and 100 pm at the medium-term (hours to days), is being prepared at VSL for traceable dimensional metrology use. Excellent vibrational and thermal stability has been achieved, essential to reaching the ambitious goals set out for the interferometer, demonstrating temperature gradients below 0.5 mK/h. Abundant laser power is made available to the interferometer by locking a tuneable diode laser to a shielded low expansion reference cavity with a 1 s standard deviation of less than 10 kHz resulting in a contribution to the measurement uncertainty of less than 2 pm. The stability of the optical components used in the interferometer was evaluated, and a powerful methodology for measuring the path length variations was implemented.
The presented double dead-path difference measurement demonstrates that the design goals for the short- and medium-term measurement uncertainty are being reached during a selected period of 19 hours, while operating in ambient air conditions. The residual pressure related path length difference fluctuations form the current limitation to the measurement uncertainty, however, a straight-forward correction algorithm to remove these fluctuations is anticipated.

REFERENCES

[1] D. Voigt, J.D. Ellis, A.L. Verlaan, R.H. Bergmans, J.W. Spronck, and R.H Munnig Schmidt, “Toward interferometry for dimensional drift measurements with nanometer uncertainty,” Meas. Sci. Technol. 22, 094029, 2011.

[2] This work receives funding within the European Metrology Research Program (EMRP), see project IND13 “Thermal design and time-dependent dimensional drift behaviour of sensors, materials and structures” (EMRP Call 2010 Industry). The EMRP is jointly funded by the EMRP participating countries within EURAMET and the European Union.

[3] J.D. Ellis, “Optical Metrology Techniques for Dimensional Stability Measurements,” Delft University of Technology, Delft, ISBN 978-94-91104-06-0, 2010.

CONTACTS

Dr. A.S. van de Nes AvandeNes@vsl.nl
Dr. D. Voigt DVoigt@vsl.nl